Measurement of the Particle Size Distribution in a Pulsed Hypersonic Flow Facility

J.W.L. Lewis,* B.P. Curry,† and D.P. Weaver‡
Calspan Field Services, Inc., Arnold Air Force Station, Tennessee

Mie scattering measurements were used to determine the mean size, particle size distribution function, and the approximate mass fraction of copper and tungsten particles in a high-enthalpy, arc-heated, short-duration flowfield. The measurement method yielded spatially-resolved results with a time resolution of approximately 10 ms. The novel aspects are presented of both the experimental and analytical methods which were used to obtain the time-dependent particle size distribution function and the particulate mass fraction.

Introduction

THE production of supersonic and hypersonic flowfields for use in ground-based aerodynamic simulation facilities invariably produces gas flows which are contaminated to greater or lesser degrees by particulate material. The nature of such particulate matter obviously depends upon the simulation facility, gas species, and the method of reservoir heating, but one can expect to find as contaminants natural atmospheric dust, erosion products from the gas heater, hydrocarbons, or, possibly, gas condensate. Further, the concentration of the particulate material in gas flowfields with arc-heater sources can be expected to be significantly higher than found in either cold-flow facilities or, perhaps, resistance-heated flows.

Although particulates may be injected into the flowfield to achieve desired aerothermal simulation capabilities, as might be required for ablation studies, the presence of particulates in the majority of simulation facilities is an undesirable feature. Not only can the presence of particulates alter significantly the single-phase gas expansion characteristics, but also the acceleration of the particles to supersonic and hypersonic speeds and the subsequent impact of particulates on aerodynamic models can affect both the heat transfer rate and turbulence structure in the vicinity of the model. Because of these possible degrading effects on the accuracy of simulation of ground-based facilities, it is desirable to determine for such flowfields the particulate size distribution function (PSDF), the knowledge of which is required for accurate two-phase flowfield calculations. However, the experimental determination of the PSDF is a nontrivial measurement problem, for, more often than not, the requirements include both time- and space-resolved results which are quite difficult to obtain with physical probes or collection plates; furthermore, the difficulties of interpretation of the results of such probes are well known. Clearly, the use of an optical method of measurement is desired and a technique which offers promise for an in situ determination of the PSDF with adequate spatial and temporal resolution is single wavelength, multiangular Mie scattering.[1,2]

This measurement method has been applied at Arnold Engineering Development Center (AEDC) for the determination of the PSDF of the flowfield of a short-duration, arc-heated wind tunnel. Specifically, the facility was the von Kármán facility (VKF) tunnel F which produced an arc-heated, Mach 13 flow of approximately 130 ms in duration. The gas phase parameters of the N_2 flowfield are measured routinely during each test run, and it was anticipated that the predominant constituents of the particulate matter in the flow were copper and tungsten, both of which are produced by vaporization of the electrode materials. Additionally, because the arc obviously is drawn before the useable flowfield is established and because the larger particulate material is removed from the flow by a swirl baffle arrangement,[3] it was expected that the PSDF would be dependent on time. Therefore, it was concluded that the Mie scattering measurements must provide a time resolution of approximately 10 ms. This article describes the experimental and analytical techniques used to accomplish this measurement, and the measured results of the PSDF and particulate mass fraction are presented.

Mie Scattering Theory and PSDF Determinations

The interaction of an incident laser beam of wavelength λ and power Φ_0 with a sample of spherical particles of size (x) and space (ℓ') distribution function $\partial n_p(x,\ell')/\partial x$ results in Mie scattered radiation. The power $\Phi_{1,2}(\Theta,\phi,\ell')$ scattered into the solid angle $\Delta\Omega$ at the spherical polar angles (Θ,ϕ) is given by

$$\Phi_{1,2}(\Theta,\phi,\eta) = \Phi_0 \int_0^{\ell} d\ell' \frac{\partial n_p}{\partial x}(x,\ell') \int_\Delta \int_\Omega d\Omega \left[\frac{d\sigma(x,\Theta,\eta)}{d\Omega}\right]_{1,2} \tag{1}$$

where $d\Omega = \sin\Theta d\Theta d\phi$ and ℓ is the observation length of the laser beam. The particle index of refraction is η, and the size parameter x and diameter D of the particle are related by $x = \pi D/\lambda$. The ordered pair subscripts $(1,2)$ of the differential cross section $d\sigma/d\Omega$ represent, respectively, the polarization components perpendicular and parallel to the scattering plane. Reference 4 presents in detail the dependence of $(d\sigma/d\Omega)_{1,2}$ on η, x, and the scattering angles (Θ,ϕ). Further, the PSDF along the laser beam, $\partial n_p(x,\ell')/\partial x$, can be written in terms of the normalized PSDF $f(x,\ell')$ as

$$\frac{\partial n_p(x,\ell')}{\partial x} = n_p(\ell') f(x,\ell') \tag{2}$$

where $n_p(\ell')$ is the local total particle number density.

For a monodisperse or a sharply-peaked PSDF an estimate of the mean diameter D $(=\lambda x/\pi)$ can be obtained, independent of $n_p(\ell')$, by forming appropriate ratios of values

Received Sept. 22, 1981; revision received April 5, 1982.

*Senior Scientist, AEDC Division; currently at University of Tennessee Space Institute.
†Physicist, PWT/ATD, AEDC Division.
‡Physicist, PWT/ATD, AEDC Division; currently at Air Force Rocket Propulsion Laboratory, Edwards, Calif.

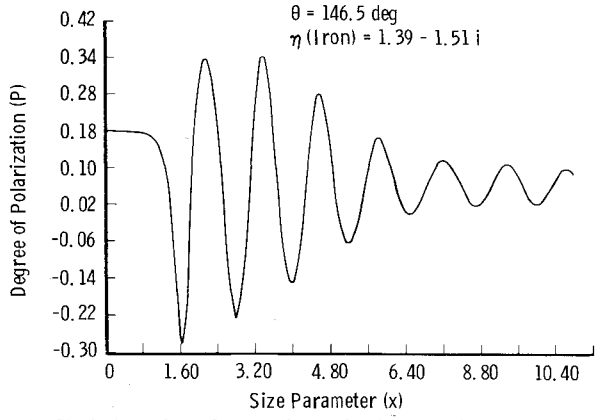

Fig. 1 Variation of the degree of polarization (P) with size parameter (x) for iron.

of the scattered flux. As an example, the degree of polarization function $P(\Theta_i,\phi_i)$ at the scattering angles (Θ_i,ϕ_i) is given by

$$P(\Theta_i,\phi_i) = [\Phi_1(\Theta_i,\phi_i) - \Phi_2(\Theta_i,\phi_i)]/[\Phi_1(\Theta_i,\phi_i) + \Phi_2(\Theta_i,\phi_i)] \quad (3)$$

The variation of P with size parameter x is shown in Fig. 1 for scattering from iron at the scattering angles $\phi = 45$ deg and $\Theta = 146.5$ deg with subtended scattering angle $\Delta\Theta = 2.65$ deg. It is seen that an experimentally-determined value of P results, in general, in ambiguous results for $\bar{x}$. Measurements of P at additional scattering angles will yield other possible solution sets for $\bar{x}$, but now the actual $\bar{x}$ for the sample must be an element of the intersection of the solution sets. Consequently, with an increase in the number of scattering angles, the ambiguity in $\bar{x}$ is reduced. However, imprecision in the experimental values of P results in a practical limitation on the reduction of the ambiguity in $\bar{x}$, and such error propagation effects are described in Ref. 2.

For those cases where limited optical access restricts the number of scattering angles and where the PSDF is a slowly varying function of position along the laser beam, two additional, n_p-independent scattering ratios ($R_{1,2}$) can be formed if the extinction (T) is measured along the laser beam path length L; viz.,

$$R_{1,2} = [\pi/\langle \sin^2\phi, \cos^2\phi \rangle] (\bar{L}/\ell) [\Phi_{1,2}(\Theta,\phi)/\Phi_0]/(-\ell n T) \quad (4)$$

where $\langle \sin^2\phi, \cos^2\phi \rangle$ represents the average of the functions over the detector solid angle and the ordering of the functions corresponds to the order of the subscript pair. The extinction factor T is defined by

$$T = \int_0^L d\ell' n_p(\ell') \int_0^\infty dx \sigma_{ext}(x) f(x)$$

where $\sigma_{ext}(x)$ is the extinction cross section[4] and the relative PSDF $f(x)$ is assumed to be independent of position. Finally, the extinction length parameter $\bar{L}$ is a distribution function weighted average of the laser path length.[2] Figure 2 shows the variation of $R_{1,2}$ with $\bar{x}$ for iron, and the reduction in the ambiguity of $\bar{x}$ by the combined use of the $P_{1,2}$ and $R_{1,2}$ ratios is indicated.

The preceding analysis can be extended to determine the mole fraction α_β and mean size $\bar{x}_\beta$ for a binary mixture ($\beta = 1,2$) of particles whose individual PSDF's are either monodisperse or sharply peaked. For such a mixture it is convenient to define a measurable polarization function P_i

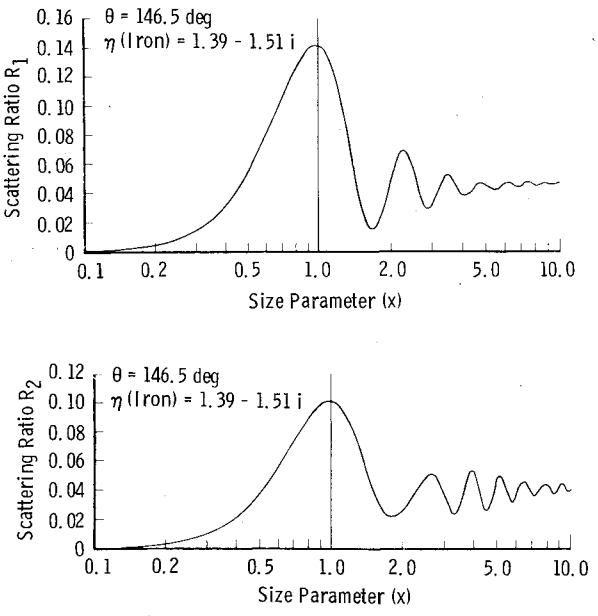

Fig. 2 Variation of scattering ratio with size parameter (x) for iron; a) scattering ratio R_1 and b) scattering ratio R_2.

for the ith pair of scattering angles (Θ_i,ϕ_i)

$$P_i = \left\{ \sum_{\beta=1}^{2} [(\Phi_1)_{i\beta} - (\Phi_2)_{i\beta}] \alpha_\beta \right\} \Big/ \left\{ \sum_{\beta=1}^{2} [(\Phi_1)_{i\beta} + (\Phi_2)_{i\beta}] \alpha_\beta \right\} \quad (5)$$

For the general overdetermined equation set represented by Eq. (5), iterative solution can be achieved for α_β and $\bar{x}_\beta$ $\beta = 1,2$, subject to the constraints $\alpha_\beta \geq 0$ and $\alpha_1 + \alpha_2 = 1$. Extension to an N-component particulate mixture is straightforward.[2]

To evaluate the accuracy of the determination of the average size parameter for single species particle samples and the average sizes and mole fractions of binary particulates, computer calculations were performed for the experimental configuration employed in this study using assumed spatially-uniform distribution functions with a range of mean size parameters and mole fractions. For the single species case, both log normal and the subsequently described two-parameter PSDF's were used. For an assumed log-normal PSDF it was found that the $\bar{x}$ value resulting from the analysis closely approximated the number median diameter of the PSDF. Similar verifications were performed for the determination of the mole fractions and mean sizes for binary mixtures of Cu and W particles.

For a single species collection of particles it is noted that Eq. (1) is of the form of an integral equation of the first kind which can, in principle, be deconvolved to determine the PSDF. Specifically, combining Eqs. (1) and (2) results in a set of integral equations relating the experimental values $\Phi_{1,2}(\Theta_i,\phi)$ to the normalized PSDF $f(x,\ell')$. The deconvolution can be performed using the constrained linear inversion method of Phillips and Twomey,[5-8] and the obtained solutions $f(x,\ell')$ are best in the sense of least-squares fitting. The work of Dave[9] and Chow and Tien[10] exemplify the use of this method.

In order to allow the determination of the relative PSDF $f(x,\ell')$ without performing absolute intensity measurements, we have modified the deconvolution procedure by using as experimental input data the ratios of the scattered power at various angles. It has been shown in Refs. 1 and 2 that it is preferable to use as a reference denominator of these ratios the polarization-unresolved scattered power at $\Theta = 90$ deg which is relatively insensitive to the nature of the PSDF.

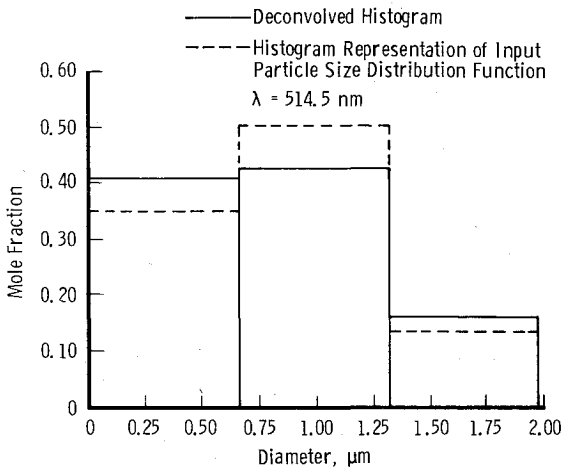

Fig. 3 Simulated deconvolution of copper particle size distribution function.

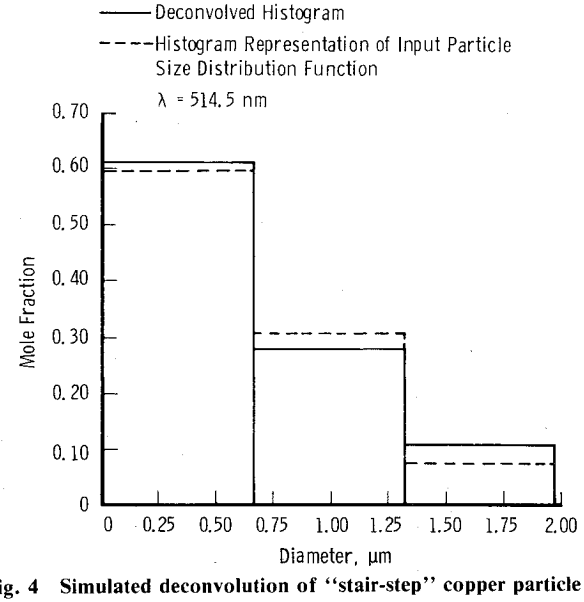

Fig. 4 Simulated deconvolution of "stair-step" copper particle size distribution function.

However, for the application of this work no optical access existed at $\Theta = 90$ deg and the reference scattered power was the sum of the polarization-unresolved signals at the two angular channels used.

To determine the accuracy of this modified deconvolution procedure, computer-generated input data were used for a wide range of PSDF's, and the resulting deconvolved PSDF was compared with the known input distribution. Using input data with no simulated experimental error provides a determination of the inaccuracy of the deconvolution procedure, and the inclusion of simulated experimental error in the input data yields an assessment of the effects of error propagation in the deconvolution. This latter case is discussed in detail in Ref. 2. Using an assumed distribution function $f(x)$ of the form

$$f(x) = C^{N+1}x^N \exp(-Cx)/N!$$

simulated PSDF deconvolutions were performed for copper particles for an "error-free" input data set which consisted of polarization-specific scattered intensities for two angular channels at $\theta = 146.5$ and 161.9 deg. Shown in Fig. 3 is a 3-bin histogram result for the case where $C = 0.746$, $N = 3.0$, and $\bar{x} = 5.36$; the dashed lines correspond to the histogram representation of the input distribution. The 3-bin simulated

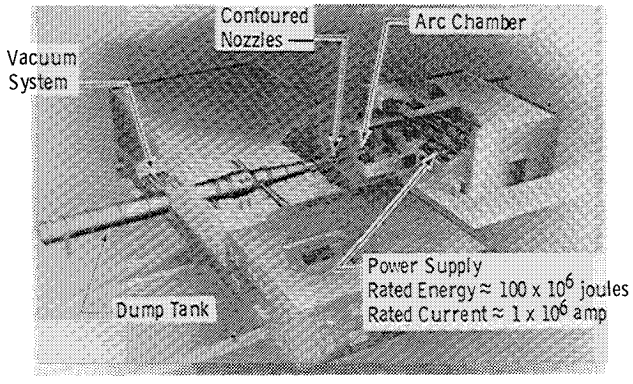

Fig. 5 AEDC-VKF tunnel F.

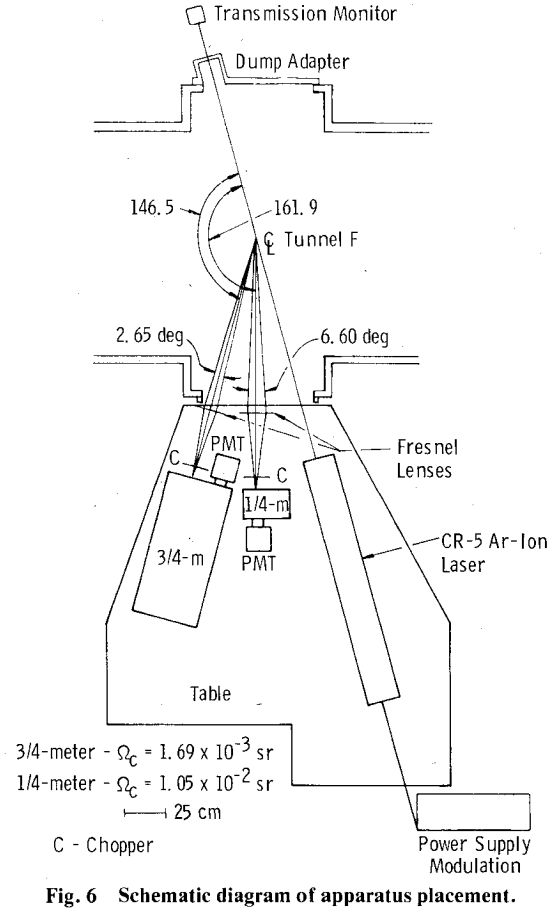

Fig. 6 Schematic diagram of apparatus placement.

deconvolution results are shown in Fig. 4. It was found that the maximum inaccuracy for the 3-bin PSDF is approximately ±20% and that 3 bins is the maximum resolution which can be obtained using this experimental configuration.

Experimental Method

The flowfield studied was produced by the AEDC von Kármán gasdynamics facility tunnel F which is an arc-heated, blow-down wind tunnel, and Fig. 5 shows the tunnel F facility. The reservoir chamber was charged to an initial pressure in the range of 14-1.4 × 10^3 atm, and the gas heated by a 10-70 ms duration arc discharge which was provided by a 280 μH, 60 MJ inductance coil. The initial arc current was in the range of 100-600 kA depending on the energy provided by the inductance coil, and approximately 50% of the source energy was deposited within the test gas. The resulting pressure increase burst the single or double diaphragm which separated the test section and reservoir, and hypersonic flow

was produced using either a Mach 8, 12, or 16 nozzle of exit diameters of 63.5 cm, 1.02 m, or 1.22 m, respectively. For this study the Mach 16 contoured nozzle was used, but aerodynamic measurements indicated that the flow Mach number was approximately Mach 13.

Figure 6 shows the experimental arrangement of the Mie scattering apparatus which was used for the measurement of the particulate properties of the Mach 13 flowfield. An unfocused, continuous argon ion laser beam of 0.62 W average power at 514.5 nm was injected diagonally across the flowfield. The power transmitted through the flowfield was measured using a coherent radiation model 212 power meter and was displayed on a Tektronix model 7633 oscilloscope, from which photographic recordings were obtained. The diagonal line-of-sight traversal distance of the beam across the 1.38-m-diam tunnel was 1.99 m. The capability existed for modulating the laser beam at 1 kHz if the spontaneous emission at 514.5 mm of the flowfield species was sufficiently large, but this was found to be unnecessary. Further, the polarization vector of the input beam was oriented so that the azimuthal scattering angle was 45 deg.

The Mie-scattered radiation from the axial centerline of the flowfield was collected by detectors which were located at the scattering angles $\Theta = 146.5$ and 161.9 deg, as shown in Fig. 6. In anticipation of the necessity of using alternate wavelengths of the Ar^+ laser because of spontaneous emission from the flowfield, spectral isolation of the RCA-31034A photomultiplier tube detectors was provided by the spectrometers shown in Fig. 5. The solid angle subtended by the detection channel at $\Theta = 146.5$ deg was 1.69×10^{-3} sr and at $\Theta = 161.9$ deg, 1.05×10^{-2} sr. Data acquisition time resolution of 10 ms was achieved for the nominal 100 ms flowfield duration using the chopper wheels shown in Fig. 7. Further, this temporal resolution was attained for each of the two perpendicular polarization states of the scattered radiation by attaching, as shown in Fig. 6, to alternate chopper wheel openings HN-22 Polaroid® material such that the polarization direction of successive slits was crossed. Each third slit was blank to provide not only a time mark reference but also an unpolarized signal. Data processing was accomplished with routine photon counting instrumentation, and data recording for the two scattering channels was achieved with dual-beam oscilloscopes.

Calibration of the system's sensitivity was performed using Rayleigh scattering measurements of air samples of known pressure and temperature. These measurements were performed both before and after the tunnel firings, and the known constituency of the air sample and the corresponding Rayleigh scattering cross sections were used to determine the system sensitivity. Depolarization measurements were also performed to ensure the absence of particulate Mie scattering effects on the calibrations.

Finally, high-speed cine photography of the Mie scattered radiation was used for visualization of the flowfield and to determine the effective transmission length [$\bar{L}$ of Eq. (4)], which could be compared with the geometric length provided by previously obtained gasdynamic measurements.

Analysis and Results

Using the methods described in previous sections, the angular scattering and extinction measurements were used to obtain time-resolved estimates of the particulate diameter, number density, and mass fraction. Potential types and sources of particles which had to be considered were copper and tungsten vaporized from the electrodes in the arc chamber, iron from the burst diaphragm and from various baffles, and H_2O droplets resulting from condensation of water vapor present in the nitrogen flow. These species were systematically investigated, and it was found that, as a single species, only copper could explain all the scattering data; and, in addition, a binary mixture of copper and tungsten was

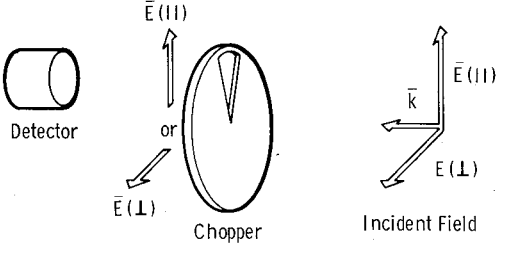

Schematic of components in optical path.

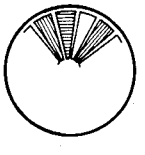

Partial view of chopper.

Fig. 7 Particle sizing detector channel configuration.

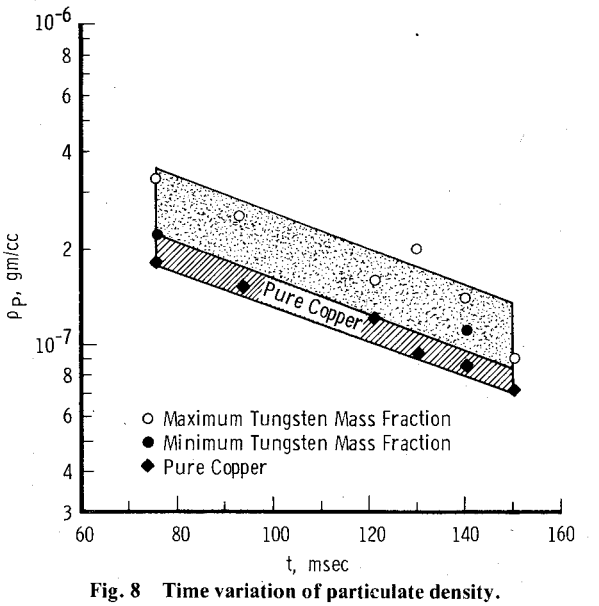

Fig. 8 Time variation of particulate density.

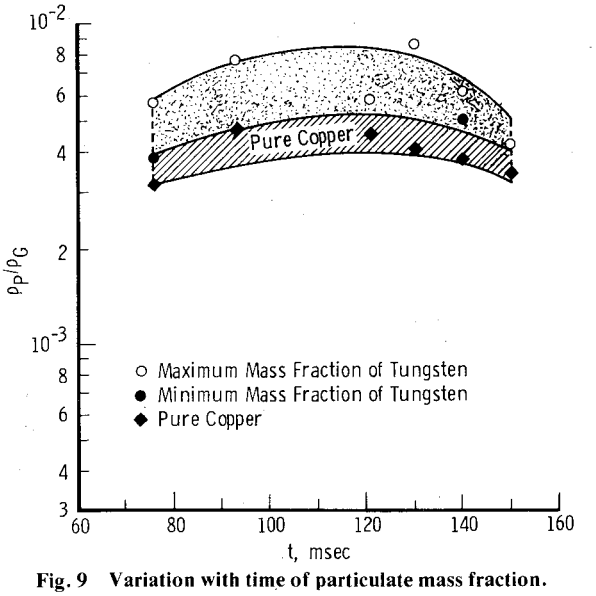

Fig. 9 Variation with time of particulate mass fraction.

found to be consistent with the scattering data. For this type of analysis, the results yielded the mole and mass fractions for each species as well as the individual species particle diameters. Additionally, the weighted-mean values for the particulate sample were obtained from the individual species values. Using an effective extinction length $\bar{L} = 132 \pm 4$ cm, which was obtained from a combination of the cine photography results, flowfield pressure measurements, and method of characteristics calculations for the flow, Fig. 8 shows the time variation of the measured particulate mass density ρ_p; time (t) is measured relative to the occurrence of the arc voltage. Since only two angular scattering channels were used, there exists an uncertainty in the results which is shown by the total shaded area of Fig. 8. It is seen that for the assumed Cu/W mixture there is an uncertainty of approximately a factor of two in the measured mass density of the mixture and that the mixture density decreases by approximately a factor of two over the duration of the run. No solutions were possible for a sample of pure tungsten. For an assumed pure copper particulate constituency, the cross-hatched region of Fig. 8 shows ρ_p to be uncertain by less than $\pm 20\%$ and to decrease from approximately 2×10^{-7} g/cc at $t \simeq 75$ ms to 8×10^{-8} g/cc at $t = 150$ ms, a factor of 2.5 decrease. Using the results shown in Fig. 8 and the time variation of the freestream N_2 density (ρ_G), the approximate particulate mass fraction was found as a function of time, and the results are shown in Fig. 9. Again, both the Cu/W mixture and the pure Cu cases are shown, and it is seen that for the duration of the flow $\rho_p/\rho_G \sim 4\text{-}5 \times 10^{-3}$.

Figure 10 shows the diameter (D_{Cu}) of Cu particles for the two assumed cases of constituency, and for all times greater than approximately 90 ms after the arc voltage, $D_{Cu} \simeq 0.90$ μm regardless of the constituency assumption. The corresponding results for the diameter of W for the mixture case showed considerably more variation (0.2-1.5 μm) for the various cases. Using these results and assuming uniformity of the particulate sample along the line-of-sight of the laser beam, the variation with time of the number density (n_p) was found, and the results are shown in Fig. 11. Although a factor of three uncertainty exists, it is seen from Fig. 11 that $n_p \sim 10^4$ cc^{-1} for the entire duration of the flow.

It is to be noted that the quoted uncertainties are the total ambiguities in the results due to both the nonmonotonic relation between the scattering ratios and the particle size parameter and the experimental imprecision ($\sim \pm 5\%$) in the scattered intensity measurements.

To determine the PSDF using the deconvolution technique described previously and by Refs. 1, 2, and 5-10 requires the assumption of a single particulate species. Figures 8-10 show that before the onset of flow breakdown at $\lambda = 168$ ms the validity of the assumption of a pure Cu particulate sample improves for the later flow times. However, as Fig. 11 indicates, the uncertainty of the data at $t = 150$ ms was believed to be too large to allow deconvolution of the data. Therefore, the data corresponding to $t = 140$ ms were used to obtain a PSDF deconvolution for an assumed pure Cu sample. The measured values of D_{Cu} as shown in Fig. 9 were used as a guide for acceptance of the deconvolution of the 3-bin histogram representation of the PSDF. Figure 12 shows the result, and the mean diameter was found to be 0.7 μm which is consistent with the result shown in Fig. 9. From Fig. 12 it is seen that more than 50% of the particles are submicron in size.§

It is of interest to use the results of these measurements to estimate the total particulate mass contained within the flowfield for the duration of the run and to compare this value with mass loss of the electrodes. For this order of

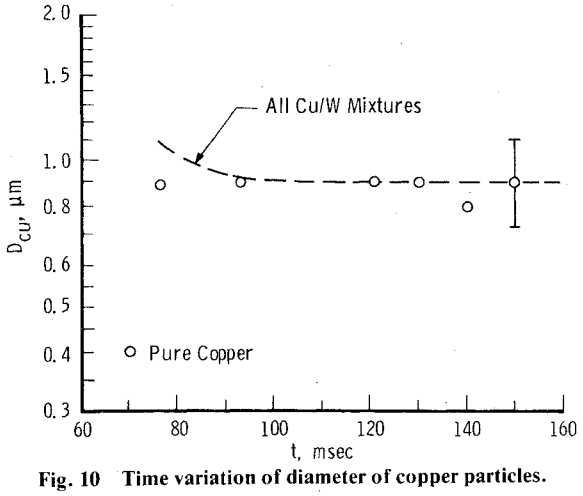

Fig. 10 Time variation of diameter of copper particles.

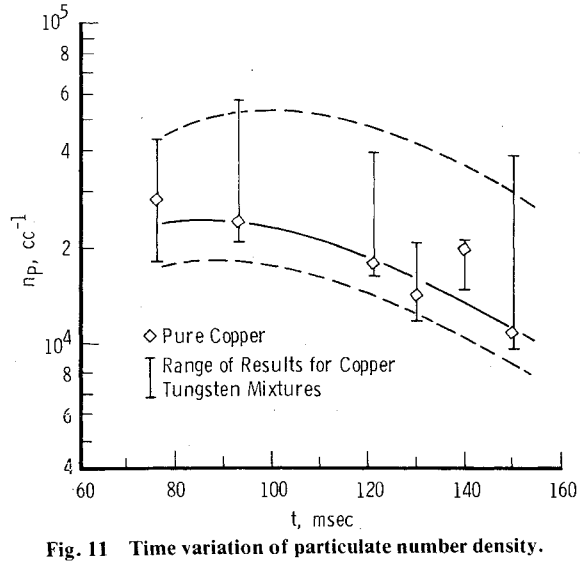

Fig. 11 Time variation of particulate number density.

magnitude calculation it is necessary to consider the possibility of the lag in speed of the particles relative to the nominal Mach 13 gas flow speed. For a particulate species of atomic species mass density ρ_s and diameter D, the characteristic time (τ_p) for the lag in particle speed relative to that of the gas is[11]

$$\tau_p \sim D\rho_s / 18\eta_v$$

where η_v is the gas viscosity. Assuming copper particles of diameter $D = 0.7\text{-}0.9$ μm, for the flowfield studied, $\tau_p \sim 10^{-4}$ s. Next, a characteristic time (τ_G) can be estimated for the gas flowfield by considering the change in gas flow speed over the length (ΔL_N) of the expansion section of the nozzle; i.e.,

$$\tau_G \sim \Delta L_N / (v_\infty - v_{th})$$

where v_∞ is the nozzle exit speed and v_{th} is the flow speed at the nozzle throat. Using values appropriate to the Mach 16 nozzle, it is found that $\tau_G \sim 5 \times 10^{-3}$ s. Therefore, the characteristic particle time τ_p is smaller than τ_G by an order of magnitude, and the particulate flow speed v_p is assumed to be equal to the freestream speed of the gas, an estimate whose uncertainty should be significantly less than an order of magnitude. Using the particulate mass density (ρ_p) results, shown in Fig. 8, and the flowfield properties of the tunnel, it is found that the particulate mass (Δm) contained within the nominal 0.1-s flowfield is on the order of 100 g. This value is

§Note added in proof: Recently we have subjected these data to further analysis using a nonlinear regression technique. The results suggest that the particles may be even smaller than shown here. The PSDF apparently can be confined within the first size bin of Fig. 12.

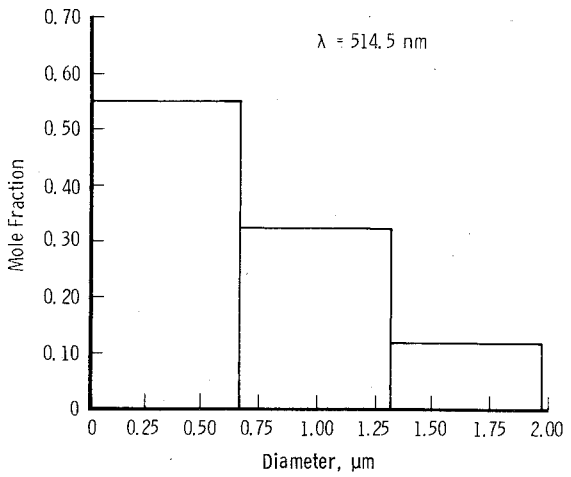

Fig. 12 Deconvolved particle size distribution function for copper particles.

to be compared with unpublished electrode mass loss measurement results of approximately 130 g.

Summary and Conclusions

Mie scattering measurements from the axial centerline region of a pulsed, arc-heated hypersonic flowfield yielded time-resolved information which was needed to characterize the particulate content of the flowfield. Because of the limited optical access to the chamber, only two, single wavelength Mie scattering channels were employed, but this information was supplemented by the use of laser beam transmission measurements and the provision for resolving the polarization states of the scattered radiation. It was necessary to assume a spatially-uniform PSDF, which, although not absolutely true, is consistent with the approximate uniformity of the gas flowfield and the expectation that submicron size particles will follow the flow. Similarly, the assumed sphericity of the particles is not believed to be at gross variance with the product of clustering and coalescence of vaporized metallic particles. With these assumptions and experimental measurements, the particulate mass density, the mass density fraction of particles in the flow, the particulate number density, and average particle diameter were found with a time resolution of 10 ms. It was found that the measurements were inexplicable if the scattering species were iron, water, or tungsten, but pure copper or copper-tungsten mixtures could yield consistent solutions. Consequently, since both copper and tungsten are products of arc-heater electrode vaporization, the analyses were performed for both cases, and, for such species constituencies, estimates of the particulate properties were obtained.

Specifically, it was found that the particulate number density (n_p), mass density (ρ_p), and mass density fraction (ρ_p/ρ_G) were approximately 10^4 cc^{-1}, 2×10^{-7} g/cc, and 5×10^{-3}, respectively. Additionally, the copper particle diameter (D_{Cu}) for both constituency cases was approximately 0.9 μm, whereas for the Cu/W mixture D_W varied from 0.2 to 1.6 μm. Further, it was found that the range of W mole fraction which was consistent with the measurements was approximately 0-20%. Finally, assuming a pure copper sample, the deconvolution of the PSDF into a 3-bin histogram representation yielded a mean particle diameter of approximately 0.7 μm and showed that over 85% of the particles were less than 1.25 μm in diameter.

In conclusion, the very limited Mie angular scattering data provided time-resolved estimates of the previously unknown characteristics of the particulate contamination of the pulsed, arc-heated flowfield. Although the uncertainties in the results are significant, the results were acceptable in view of the previous knowledge of the parameters, and, finally, improvements in the experimental configuration and resulting accuracy are possible.

References

[1]Lewis, J. W. L., Curry, B. P., and Weaver, D. P., "Determination of the Size Distribution Function for Particles in a Hypersonic Flow Field," AEDC-TR-77-101 (AD-A056923), July 1978.

[2]Curry, B. P., Weaver, D. P., and Lewis, J. W. L., "Development of Mie Scattering Techniques for In-Situ Particle Diagnostics at AEDC," AEDC-TR-80-3 (AD-A092716), Nov. 1980.

[3]Wagner, D. A., "Development of a Centrifugal Particle Separator for Hotshot Wind Tunnels," AEDC-TR-74-55, Aug. 1974.

[4]Kerker, M., *The Scattering of Light and Other Electromagnetic Radiation,* Academic Press, New York, 1969.

[5]Philips, D. L., "A Technique for the Numerical Solution of Certain Integral Equations of the First Kind," *Journal of the Association for Computing Machinery,* Vol. 9, Jan. 1962, pp. 84-97.

[6]Twomey, S., "On the Numerical Solution of the Fredholm Integral Equations of the First Kind by the Inversion of the Linear System Produced by Quadrature," *Journal of the Association for Computing Machinery,* Vol. 10, Jan. 1963, pp. 97-101.

[7]Twomey, S., "The Application of Numerical Filtering to the Solution of the Integral Equations Encountered in Indirect Sensing Measurements," *Journal of the Franklin Institute,* Vol. 279, Jan. 1965, pp. 95-109.

[8]Twomey, S. and Howell, H. B., "Some Aspects of the Optical Estimation of Microstructure in Fog and Cloud," *Applied Optics,* Vol. 6, Dec. 1967, p. 2129.

[9]Dave, J. V., "Determination of Size Distribution of Spherical Polydispersions Using Scattered Radiation Data," *Applied Optics,* Vol. 10, Sept. 1971, pp. 2035-2044.

[10]Chow, L. C. and Tien, D. L., "Inversion Technique for Determining the Droplet Size Distribution in Clouds: Numerical Examination," *Applied Optics,* Vol. 15, Feb. 1976, pp. 378-383.

[11]Rudinger, G., "Relaxation in Gas-Particle Flow" *Nonequilibrium Flows,* edited by P. Wegner, Marcel Dekker, Inc., New York, 1969.